



Creep instability analysis of viscoelastic sandwich shell panels

Nasrin Jafari¹ · Mojtaba Azhari¹

Received: 23 December 2023 / Accepted: 2 February 2024 / Published online: 13 February 2024
© The Author(s), under exclusive licence to Springer Nature B.V. 2024

Abstract

This paper considers the creep instability analysis of time-dependent sandwich cylindrical and spherical shell panels of quadrilateral planforms having elastic faces and viscoelastic cores according to the first-order shear deformation theory. The viscoelastic properties of the core are extracted based on the Boltzmann integral law. The equilibrium equation is expressed utilizing the virtual work principle. The space and time parts of the displacement vector are approximated using the simple HP-cloud mesh-free method (which has H refinement and P enrichment properties), and the exponential time function, respectively. The stiffness and geometry matrices are constructed in the Laplace–Carson domain. Finally, the time behavior of viscoelastic sandwich shell panels under in-plane compressions is predicted by solving the eigenvalue problem in the Laplace–Carson domain. Also, the maximum compressive load is determined which can be applied to the time-dependent sandwich shell panels without any creep instability. This critical compression is less than the buckling load of the viscoelastic sandwich shell panel at time zero.

Keywords Creep instability analysis · Time function · Time-dependent core · Viscoelastic sandwich shell panels

1 Introduction

Recently the employment of sandwich shell panels with viscoelastic cores has increased in various advanced industries. These structures possess some good mechanical characteristics such as lightweight, high bending stiffness, and good damping. Therefore, engineers need to know about viscoelastic sandwich shell instability conditions.

On the other hand, creep instability analysis is one of the important parameters in designing viscoelastic shells. Creep instability is a critical condition of viscoelastic structures in which the deflections diverge to infinity as time increases. The viscoelastic instability or creep instability is related to the ratio of applied in-plane compressive load to the elastic buckling load at time zero, and time-dependent viscoelastic material property, too.

Some papers have considered the buckling analysis of shells, while other papers have investigated the thermal buckling analysis of viscoelastic shells. Ishakov (1999) analyzed

✉ N. Jafari
jafarin@iut.ac.ir

¹ Department of Civil Engineering, Isfahan University of Technology, Isfahan 84156-83111, Iran

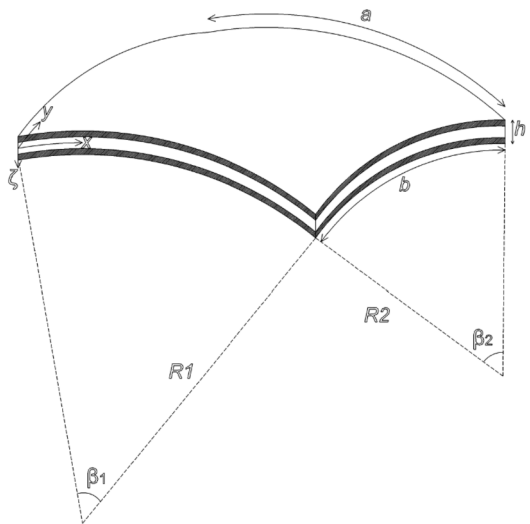
the stability of viscoelastic flexible thin shallow hyperbolic paraboloid shells subjected to transversal loads considering the initial imperfection and geometrical nonlinearity. Ferreira and Barbosa (2000) presented the stability analysis of orthotropic composite shell structures based on the finite element method. Pradeep et al. (2006) studied the stability and vibration analysis of viscoelastic sandwich cylinders with viscoelastic cores under the thermal environment utilizing the semianalytical finite element method. Ganesan and Sethuraman (2007) considered the buckling and free vibration analysis of sandwich general shells of revolution under the thermal environment employing the semianalytical finite element method. Mahmoudkhani et al. (2016) considered the aero-thermo-elastic stability of sandwich cylindrical shells with viscoelastic cores in supersonic airflow based on the von Karman–Donnell kinematic nonlinearity. Li and Liu (2022) investigated the thermal buckling and free vibration analysis of viscoelastic functionally graded sandwich shells with tunable auxetic honeycomb cores.

Also, several papers have studied the dynamic buckling analysis of viscoelastic shells. Tylikowski (1989) studied the dynamic stability analysis of Voigt–Kelvin viscoelastic cylindrical circular shells under time-dependent membrane loads. Drozdov (1993) presented the dynamic stability analysis of viscoelastic cylindrical shells subjected to periodic and stochastic loadings. Hajmohammad et al. (2018) investigated the dynamic buckling analysis of multiphase nanocomposite viscoelastic laminated conical shells under moisture, temperature, and magnetic loads. Al-Furjan et al. (2020) considered the dynamic buckling analysis of viscoelastic carbon nano cones subjected to magnetic and thermal loads based on the higher-order nonlocal viscoelastic strain gradient theory. Biswal and Mohanty (2020) investigated the free vibration and stability analysis of doubly curved laminated composite spherical sandwich shell panels with viscoelastic cores subjected to uniaxial and biaxial harmonic excitations based on the Sander’s approximation.

Some other papers have considered the creep buckling analysis of viscoelastic shells. Davidson and Browning (1964) studied the creep buckling analysis of axially compressed cylindrical shells with viscoelastic cores. Vinogradov (1986) presented the creep-stability analysis of viscoelastic cylindrical shells subjected to axial compressions. Peng et al. (2007) considered the critical buckling load of viscoelastic laminated circular cylindrical shells under axial compressions within the theory of classic buckling based on the Boltzmann hereditary integral. Liu et al. (2022) studied the time-dependent buckling analysis of linear viscoelastic spherical shells based on the small-strain and moderate-rotation shell theory. Xu et al. (2022) investigated the creep buckling analysis of acrylic glass pressure cylindrical shells experimentally and compared the results with the finite element simulation. Jafari and Azhari (2022) considered the time-dependent instability analysis of Timoshenko viscoelastic beams and moderately thick viscoelastic plates under compressive loads based on the Boltzmann integral law.

Following the work presented by Jafari and Azhari (2022) in which the viscoelastic instability analysis of time-dependent Timoshenko beams and Mindlin plates was introduced, in this paper the creep instability analysis of sandwich shell panels with viscoelastic cores is considered. The stress-strain relations are written based on the Boltzmann integral law with time-dependent shear modulus and constant bulk modulus. The displacement vector is separated by a product of a geometrical function and a time function. Space discretization is based on the simple HP-cloud mesh-free method. By solving an eigenvalue problem in the Laplace–Carson domain the solution is completed. Consequently, the time behavior of viscoelastic sandwich shell panels subjected to in-plane compressions is formulated for the first time. Besides, the maximum compression is determined which can be applied to the viscoelastic sandwich shell panels, without any creep instability. Many numerical results are

Fig. 1 A moderately thick three-layer sandwich shell panel



studied to obtain the effects of geometrical and material parameters on the time-dependent instability analysis of moderately thick viscoelastic sandwich shell panels.

This paper is organized as follows: The formulations are extracted in Sect. 2. Numerical results and conclusions are presented in Sects. 3 and 4, respectively.

2 Governing equations

2.1 Kinematic of the shell

By investigating a moderately thick three-layer sandwich shell panel of quadrilateral plan-form with two elastic faces and the viscoelastic core having the radii R_1 and R_2 , shell angles β_1 and β_2 , total thickness h , length a , and width b , as shown in Fig. 1, the first-order shear deformation theory (FSDT) of displacement field can be expressed as (Reddy 2004):

$$\begin{Bmatrix} u(x, y, \zeta) \\ v(x, y, \zeta) \\ w(x, y, \zeta) \end{Bmatrix} = \begin{Bmatrix} u_0(x, y) + \zeta \varphi_x(x, y) \\ v_0(x, y) + \zeta \varphi_y(x, y) \\ w_0(x, y) \end{Bmatrix}, \tag{1}$$

where u , v , and w represent the displacements in the longitudinal, tangential, and radial directions, respectively. Also φ_x and φ_y represent the rotations of the midplane about the y and x axes, respectively; ζ is measured from the midplane, and u_0 , v_0 , and w_0 are the displacements of the middle surface.

The vector of in-plane $\boldsymbol{\varepsilon}_0$, nonlinear $\boldsymbol{\varepsilon}_{NL}$, bending $\boldsymbol{\kappa}$, and shear $\boldsymbol{\Gamma}$ strain–displacement can be stated as:

$$\boldsymbol{\varepsilon}_0(x, y) = \begin{Bmatrix} \frac{\partial u_0}{\partial x} + \frac{w_0}{R_1} \\ \frac{\partial v_0}{\partial y} + \frac{w_0}{R_2} \\ \frac{\partial v_0}{\partial x} + \frac{\partial u_0}{\partial y} \end{Bmatrix}, \boldsymbol{\varepsilon}_{NL}(x, y) = \begin{Bmatrix} \frac{1}{2} \left(\frac{\partial w_0}{\partial x} \right)^2 \\ \frac{1}{2} \left(\frac{\partial w_0}{\partial y} \right)^2 \\ \frac{\partial w_0}{\partial x} \frac{\partial w_0}{\partial y} \end{Bmatrix}, \boldsymbol{\kappa}(x, y) = \begin{Bmatrix} \frac{\partial \varphi_x}{\partial x} \\ \frac{\partial \varphi_y}{\partial y} \\ \frac{\partial \varphi_y}{\partial x} + \frac{\partial \varphi_x}{\partial y} \end{Bmatrix}, \tag{2}$$

$$\boldsymbol{\Gamma}(x, y) = \begin{Bmatrix} \frac{\partial w_0}{\partial x} + \varphi_x - \frac{u_0}{R_1} \\ \frac{\partial w_0}{\partial y} + \varphi_y - \frac{v_0}{R_2} \end{Bmatrix}.$$

2.2 Constitutive relations

By considering the sandwich shell panel which is made of two symmetrical isotropic elastic face layers with the thickness h_f and the isotropic viscoelastic core layer with the thickness h_c , the stress–strain relations of the face layers, and the time-dependent core layer according to the Boltzmann integral law, are given by:

$$\boldsymbol{\sigma}_f(x, y, \zeta) = \mathbf{C}_f \boldsymbol{\varepsilon}_f(x, y, \zeta), \quad \mathbf{C}_f = \begin{bmatrix} \mathbf{C}_b^f & \mathbf{0} \\ \mathbf{0} & \mathbf{C}_s^f \end{bmatrix}, \tag{3}$$

$$\boldsymbol{\sigma}_c(x, y, \zeta, t) = \mathbf{C}_c(t) \boldsymbol{\varepsilon}_c(x, y, \zeta, t = 0) + \int_0^t \mathbf{C}_c(t - \tau) \dot{\boldsymbol{\varepsilon}}_c(x, y, \zeta, \tau) d\tau, \tag{4}$$

$$\dot{\boldsymbol{\varepsilon}}_c = \frac{\partial \boldsymbol{\varepsilon}_c}{\partial t}, \quad \mathbf{C}_c(t) = \begin{bmatrix} \mathbf{C}_b^c(t) & \mathbf{0} \\ \mathbf{0} & \mathbf{C}_s^c(t) \end{bmatrix},$$

where t represents the time, $\boldsymbol{\sigma}_f(x, y, \zeta)$ and $\boldsymbol{\varepsilon}_f(x, y, \zeta)$ are the stress and strain vectors of face layers; $\boldsymbol{\sigma}_c(x, y, \zeta, t)$ and $\boldsymbol{\varepsilon}_c(x, y, \zeta, t)$ are the stress and strain vectors of the time-dependent core layer. Also, the bending \mathbf{C}_b^f , $\mathbf{C}_b^c(t)$ and shear \mathbf{C}_s^f , $\mathbf{C}_s^c(t)$ modulus tensors of elastic faces and the viscoelastic core are obtained as:

$$\mathbf{C}_b^f = \frac{E_f}{(1 - \nu_f^2)} \begin{bmatrix} 1 & \nu_f & 0 \\ \nu_f & 1 & 0 \\ 0 & 0 & \frac{1 - \nu_f}{2} \end{bmatrix}, \quad \mathbf{C}_s^f = \frac{E_f}{2(1 + \nu_f)} \begin{bmatrix} 1 & 0 \\ 0 & 1 \end{bmatrix}, \tag{5}$$

$$\mathbf{C}_b^c(t) = \frac{E_c(t)}{(1 - \nu_c^2(t))} \begin{bmatrix} 1 & \nu_c(t) & 0 \\ \nu_c(t) & 1 & 0 \\ 0 & 0 & \frac{1 - \nu_c(t)}{2} \end{bmatrix}, \quad \mathbf{C}_s^c(t) = \frac{E_c(t)}{2(1 + \nu_c(t))} \begin{bmatrix} 1 & 0 \\ 0 & 1 \end{bmatrix}, \tag{6}$$

where E_f and ν_f are the elasticity modulus and Poisson ratio of the face layers, and $E_c(t)$ and $\nu_c(t)$ are the time-dependent elasticity modulus and Poisson ratio of the core layer, respectively.

Assuming the constant bulk modulus K_c and the time-dependent shear modulus $G_c(t)$, the bulk and shear moduli of the viscoelastic core can be expressed as (Eskandari et al. 2022)

$$K_c(t) = K_c, G_c(t) = G_1 + G_2 e^{-\frac{t}{t_s}}, \tag{7}$$

where G_1 and G_2 are constants, and t_s is the relaxation time of a viscoelastic material.

The time-dependent shear modulus can be rewritten as follows:

$$G_c(t) = \frac{3}{2} K_c \left(c_1 + c_2 e^{-\frac{t}{\tau}} \right) = \frac{3}{2} K_c \omega(t), \quad \omega(t) = c_1 + c_2 e^{-\frac{t}{\tau}}, \tag{8}$$

in which c_1 and c_2 are constant coefficients, and $\omega(t)$ is the relaxation function of a viscoelastic material.

Using relations

$$K_c(t) = \frac{E_c(t)}{3(1 - 2\nu_c(t))}, \quad G_c(t) = \frac{E_c(t)}{2(1 + \nu_c(t))}, \tag{9}$$

the time-dependent elasticity modulus $E_c(t)$ and Poisson ratio $\nu_c(t)$ can be stated as:

$$E_c(t) = \frac{9K_c\omega(t)}{2 + \omega(t)}, \quad \nu_c(t) = \frac{1 - \omega(t)}{2 + \omega(t)}. \tag{10}$$

2.3 Integrating over the shell thickness

By integrating over the thickness of the three-layer symmetrical viscoelastic sandwich shell, the in-plane $\mathbf{D}_p(t)$, bending $\mathbf{D}_b(t)$, and shear $\mathbf{D}_s(t)$ modulus tensors are obtained as:

$$\begin{aligned} \mathbf{D}_p(t) &= 2h_f \mathbf{C}_b^f + h_c \mathbf{C}_b^c(t), \quad \mathbf{D}_b(t) = \frac{2}{3} h_e \mathbf{C}_b^f + \frac{h_c^3}{12} \mathbf{C}_b^c(t), \\ \mathbf{D}_s(t) &= k(2h_f \mathbf{C}_s^f + h_c \mathbf{C}_s^c(t)), \end{aligned} \tag{11}$$

in which k is the shear correction factor related to the FSDT and

$$h_e = 1.5h_c h_f^2 + 0.75h_c^2 h_f + h_f^3. \tag{12}$$

Thus, the time-dependent resultant vectors of in-plane force $\mathbf{N}(t)$, bending moment $\mathbf{M}(t)$, and shear force $\mathbf{Q}(t)$ are obtained as follows:

$$\begin{aligned} \mathbf{N}(x, y, t) &= \mathbf{D}_p(t) \boldsymbol{\varepsilon}_0(0) + \int_0^t \mathbf{D}_p(t - \tau) \dot{\boldsymbol{\varepsilon}}_0(x, y, \tau) d\tau, \quad \dot{\boldsymbol{\varepsilon}}_0(x, y, t) = \frac{\partial \boldsymbol{\varepsilon}_0(x, y, t)}{\partial t}, \\ \mathbf{M}(x, y, t) &= \mathbf{D}_b(t) \boldsymbol{\kappa}(0) + \int_0^t \mathbf{D}_b(t - \tau) \dot{\boldsymbol{\kappa}}(x, y, \tau) d\tau, \quad \dot{\boldsymbol{\kappa}}(x, y, t) = \frac{\partial \boldsymbol{\kappa}(x, y, t)}{\partial t}, \\ \mathbf{Q}(x, y, t) &= \mathbf{D}_s(t) \boldsymbol{\Gamma}(0) + \int_0^t \mathbf{D}_s(t - \tau) \dot{\boldsymbol{\Gamma}}(x, y, \tau) d\tau, \quad \dot{\boldsymbol{\Gamma}}(x, y, t) = \frac{\partial \boldsymbol{\Gamma}(x, y, t)}{\partial t}. \end{aligned} \tag{13}$$

In the above equations, $\boldsymbol{\varepsilon}_0(0) = \boldsymbol{\varepsilon}_0(x, y, t = 0)$, $\boldsymbol{\kappa}(0) = \boldsymbol{\kappa}(x, y, t = 0)$, $\boldsymbol{\Gamma}(0) = \boldsymbol{\Gamma}(x, y, t = 0)$.

2.4 Virtual work principle

Utilizing the virtual work principle, the equilibrium equation of a viscoelastic sandwich shell panel subjected to in-plane compressive loads N_x and N_y can be expressed as

$$\delta U - \delta V = 0. \tag{14}$$

The variations of the strain U and potential V energies are given by:

$$\begin{aligned} \delta U = & \left(\int_V \boldsymbol{\varepsilon}_0^T(0) \mathbf{D}_p(t) \delta \boldsymbol{\varepsilon}_0 dA + \int_A \int_0^t \dot{\boldsymbol{\varepsilon}}_0^T(\tau) \mathbf{D}_p(t-\tau) d\tau \delta \boldsymbol{\varepsilon}_0 dA \right) \\ & + \left(\int_A \boldsymbol{\kappa}^T(0) \mathbf{D}_b(t) \delta \boldsymbol{\kappa} dA + \int_A \int_0^t \dot{\boldsymbol{\kappa}}^T(\tau) \mathbf{D}_b(t-\tau) d\tau \delta \boldsymbol{\kappa} dA \right) \end{aligned} \quad (15)$$

$$\begin{aligned} & + \left(\int_A \boldsymbol{\Gamma}^T(0) \mathbf{D}_s(t) \delta \boldsymbol{\Gamma} dA + \int_A \int_0^t \dot{\boldsymbol{\Gamma}}^T(\tau) \mathbf{D}_s(t-\tau) d\tau \delta \boldsymbol{\Gamma} dA \right), \\ \delta V = & \int_A \left(N_x \frac{\partial w_0}{\partial x} \frac{\partial \delta w_0}{\partial x} + N_y \frac{\partial w_0}{\partial y} \frac{\partial \delta w_0}{\partial y} \right) dA. \end{aligned} \quad (16)$$

2.5 Separation of variables

The displacement vector of a Mindlin time-dependent sandwich shell panel may be approximated using the separation of variables method as follows (Jafari and Azhari 2022; Jafari 2022)

$$\mathbf{u}(x, y, t) = \begin{Bmatrix} u_0(x, y, t) \\ v_0(x, y, t) \\ w_0(x, y, t) \\ \varphi_x(x, y, t) \\ \varphi_y(x, y, t) \end{Bmatrix} = \begin{Bmatrix} u_0(x, y) \\ v_0(x, y) \\ w_0(x, y) \\ \varphi_x(x, y) \\ \varphi_y(x, y) \end{Bmatrix} F(t) = \mathbf{u}^{xy} F(t), \quad \mathbf{u}^{xy} = \begin{Bmatrix} u_0(x, y) \\ v_0(x, y) \\ w_0(x, y) \\ \varphi_x(x, y) \\ \varphi_y(x, y) \end{Bmatrix}. \quad (17)$$

The time function $F(t)$ may be approximated as

$$F(t) = e^{s_1 t}, \quad (18)$$

where s_1 is an unknown coefficient which must be calculated.

The variations of displacement vectors and the rates of displacement vectors can be given by:

$$\delta \boldsymbol{\varepsilon}_0(x, y) = \boldsymbol{\varepsilon}_0^{xy} \delta F, \quad \delta \boldsymbol{\kappa}(x, y) = \boldsymbol{\kappa}^{xy} \delta F, \quad \delta \boldsymbol{\Gamma}(x, y) = \boldsymbol{\Gamma}^{xy} \delta F, \quad (19)$$

$$\dot{\boldsymbol{\varepsilon}}_0(x, y, t) = \boldsymbol{\varepsilon}_0^{xy} \dot{F}(t), \quad \dot{\boldsymbol{\kappa}}(x, y, t) = \boldsymbol{\kappa}^{xy} \dot{F}(t), \quad \dot{\boldsymbol{\Gamma}}(x, y, t) = \boldsymbol{\Gamma}^{xy} \dot{F}(t). \quad (20)$$

2.6 Discretizing equations

The space displacement vector can be discretized by employing the simple HP-cloud method (Jafari and Azhari 2017) as:

$$\mathbf{u}^{xy} = \mathbf{N}(x, y) \mathbf{U}^{xy}, \quad \mathbf{U}^{xy} = [\mathbf{U}_1^T \quad \mathbf{U}_2^T \quad \dots \quad \mathbf{U}_N^T], \quad (21)$$

in which \mathbf{U}_i is defined as follows:

$$\mathbf{U}_i = \langle u_{0i} \quad v_{0i} \quad w_{0i} \quad \varphi_{xi} \quad \varphi_{yi} \rangle^T, \quad i = 1 : N. \quad (22)$$

Substituting Eqs. (17)–(22) into Eqs. (15)–(16) yields

$$\delta U = \left(\int_A \mathbf{U}^{xyT} \mathbf{B}_p^T F(0) \mathbf{D}_p(t) \mathbf{B}_p \mathbf{U}^{xy} \delta F dA \right)$$

$$\begin{aligned}
 & + \int_A \int_0^t \mathbf{U}^{xyT} \mathbf{B}_p^T \dot{F}(\tau) \mathbf{D}_p(t - \tau) d\tau \mathbf{B}_p \mathbf{U}^{xy} \delta F dA \\
 & + \left(\int_A \mathbf{U}^{xyT} \mathbf{B}_b^T F(0) \mathbf{D}_b(t) \mathbf{B}_b \mathbf{U}^{xy} \delta F dA \right. \\
 & \left. + \int_A \int_0^t \mathbf{U}^{xyT} \mathbf{B}_b^T \dot{F}(\tau) \mathbf{D}_b(t - \tau) d\tau \mathbf{B}_b \mathbf{U}^{xy} \delta F dA \right) \tag{23} \\
 & + \left(\int_A \mathbf{U}^{xyT} \mathbf{B}_s^T F(0) \mathbf{D}_s(t) \mathbf{B}_s \mathbf{U}^{xy} \delta F dA \right. \\
 & \left. + \int_A \int_0^t \mathbf{U}^{xyT} \mathbf{B}_s^T \dot{F}(\tau) \mathbf{D}_s(t - \tau) d\tau \mathbf{B}_s \mathbf{U}^{xy} \delta F dA \right) \\
 & = \mathbf{U}^{xyT} \int_A \left(\mathbf{B}_p^T \left(F(0) \mathbf{D}_p(t) + \int_0^t \dot{F}(\tau) \mathbf{D}_p(t - \tau) d\tau \right) \mathbf{B}_p \right. \\
 & \quad + \mathbf{B}_b^T \left(F(0) \mathbf{D}_b(t) + \int_0^t \dot{F}(\tau) \mathbf{D}_b(t - \tau) d\tau \right) \mathbf{B}_b \\
 & \quad \left. + \mathbf{B}_s^T \left(F(0) \mathbf{D}_s(t) + \int_0^t \dot{F}(\tau) \mathbf{D}_s(t - \tau) d\tau \right) \mathbf{B}_s \right) dA \delta F \mathbf{U}^{xy}, \\
 \delta V & = \int_A \mathbf{U}^{xyT} \mathbf{B}_G^T F(t) \mathbf{N}_p \mathbf{B}_G \mathbf{U}^{xy} \delta F dA = \mathbf{U}^{xyT} F(t) \left(\int_A \mathbf{B}_G^T \mathbf{N}_p \mathbf{B}_G dA \right) \delta F \mathbf{U}^{xy}, \tag{24}
 \end{aligned}$$

where \mathbf{N}_p is the matrix of in-plane compressive forces as follows:

$$\mathbf{N}_p = \begin{bmatrix} N_x & 0 \\ 0 & N_y \end{bmatrix} = \alpha_1 N_{cr} \begin{bmatrix} k_1 & 0 \\ 0 & k_2 \end{bmatrix}, \quad k_1 = \frac{N_x}{N_{cr}}, \quad k_2 = \frac{N_y}{N_{cr}}, \quad |\alpha_1| < 1, \tag{25}$$

where N_{cr} is the buckling load of a viscoelastic sandwich shell panel at time zero, and α_1 is the arbitrary constant coefficient.

Other parameters in Eqs. (23)–(24) are defined as:

$$\begin{aligned}
 \mathbf{B}_p^i & = \begin{bmatrix} \mathbf{N}_{,x}^i & 0 & \mathbf{N}^i/R_1 & 0 & 0 \\ \mathbf{N}_{,y}^i & \mathbf{N}_{,x}^i & \mathbf{N}^i/R_2 & 0 & 0 \\ \mathbf{N}_{,y}^i & \mathbf{N}_{,x}^i & 0 & 0 & 0 \end{bmatrix}, & \mathbf{B}_b^i & = \begin{bmatrix} 0 & 0 & 0 & \mathbf{N}_{,x}^i & 0 \\ 0 & 0 & 0 & 0 & \mathbf{N}_{,y}^i \\ 0 & 0 & 0 & \mathbf{N}_{,y}^i & \mathbf{N}_{,x}^i \end{bmatrix}, \\
 \mathbf{B}_s^i & = \begin{bmatrix} \frac{-\mathbf{N}^i}{R_1} & 0 & \mathbf{N}_{,x}^i & \mathbf{N}^i & 0 \\ 0 & \frac{-\mathbf{N}^i}{R_2} & \mathbf{N}_{,y}^i & 0 & \mathbf{N}^i \end{bmatrix}, & \mathbf{B}_G^i & = \begin{bmatrix} 0 & 0 & \mathbf{N}_{,x}^i & 0 & 0 \\ 0 & 0 & \mathbf{N}_{,y}^i & 0 & 0 \end{bmatrix}.
 \end{aligned} \tag{26}$$

Substituting Eqs. (23)–(24) into Eq. (14) gives

$$\begin{aligned}
 & \left\{ \mathbf{U}^{xyT} \left(\int_A \left(\mathbf{B}_p^T \left(F(0) \mathbf{D}_p(t) + \int_0^t \dot{F}(\tau) \mathbf{D}_p(t - \tau) d\tau \right) \mathbf{B}_p \right. \right. \right. \\
 & \quad + \mathbf{B}_b^T \left(F(0) \mathbf{D}_b(t) + \int_0^t \dot{F}(\tau) \mathbf{D}_b(t - \tau) d\tau \right) \mathbf{B}_b \\
 & \quad \left. \left. + \mathbf{B}_s^T \left(F(0) \mathbf{D}_s(t) + \int_0^t \dot{F}(\tau) \mathbf{D}_s(t - \tau) d\tau \right) \mathbf{B}_s \right) dA \right) \mathbf{U}^{xy} \right. \\
 & \tag{27}
 \end{aligned}$$

$$- \mathbf{U}^{xyT} \left(\int_A \mathbf{B}_G^T F(t) \mathbf{N}_p \mathbf{B}_G dA \right) \mathbf{U}^{xy} \} \delta F = 0.$$

Removing $\delta F \neq 0$ from Eq. (27) yields

$$\begin{aligned} & \mathbf{U}^{xyT} \left(\int_A \left(\mathbf{B}_p^T \left(F(0) \mathbf{D}_p(t) + \int_0^t \dot{F}(\tau) \mathbf{D}_p(t-\tau) d\tau \right) \mathbf{B}_p \right. \right. \\ & \quad + \mathbf{B}_b^T \left(F(0) \mathbf{D}_b(t) + \int_0^t \dot{F}(\tau) \mathbf{D}_b(t-\tau) d\tau \right) \mathbf{B}_b \\ & \quad \left. \left. + \mathbf{B}_s^T \left(F(0) \mathbf{D}_s(t) + \int_0^t \dot{F}(\tau) \mathbf{D}_s(t-\tau) d\tau \right) \mathbf{B}_s \right) dA \right) \mathbf{U}^{xy} \\ & - \mathbf{U}^{xyT} \left(\int_A \mathbf{B}_G^T F(t) \mathbf{N}_p \mathbf{B}_G dA \right) \mathbf{U}^{xy} = 0. \end{aligned} \quad (28)$$

2.7 Transforming to the Laplace domain

Using the Laplace transform, we obtain

$$\begin{aligned} & \mathbf{U}^{xyT} \left(\left(\int_A \mathbf{B}_p^T s \mathbf{D}_p^* F^* \mathbf{B}_p dA + \int_A \mathbf{B}_b^T s \mathbf{D}_b^* F^* \mathbf{B}_b dA + \int_A \mathbf{B}_s^T s \mathbf{D}_s^* F^* \mathbf{B}_s dA \right) \right. \\ & \quad \left. - \left(\int_A \mathbf{B}_G^T F^* \mathbf{N}_p \mathbf{B}_G dA \right) \right) \mathbf{U}^{xy} = 0, \end{aligned} \quad (29)$$

in which F^* , \mathbf{D}_p^* , \mathbf{D}_b^* , and \mathbf{D}_s^* are the Laplace transformation of $F(t)$, $\mathbf{D}_p(t)$, $\mathbf{D}_b(t)$, and $\mathbf{D}_s(t)$, respectively. Equation (29) can be rewritten as

$$\begin{aligned} & \mathbf{U}^{xyT} \left(\int_A \mathbf{B}_p^T \bar{\mathbf{D}}_p \mathbf{B}_p dA + \int_A \mathbf{B}_b^T \bar{\mathbf{D}}_b \mathbf{B}_b dA + \int_A \mathbf{B}_s^T \bar{\mathbf{D}}_s \mathbf{B}_s dA \right. \\ & \quad \left. - \int_A \mathbf{B}_G^T \mathbf{N}_p \mathbf{B}_G dA \right) F^* \mathbf{U}^{xy} = 0, \\ & \bar{\mathbf{D}}_p = s \mathbf{D}_p^*, \quad \bar{\mathbf{D}}_b = s \mathbf{D}_b^*, \quad \bar{\mathbf{D}}_s = s \mathbf{D}_s^*. \end{aligned} \quad (30)$$

The Laplace–Carson transforms of in-plane, bending, and shear effective modulus tensors can be defined as:

$$\bar{\mathbf{D}}_p = 2h_f \mathbf{C}_b^f + h_c \bar{\mathbf{C}}_b^c, \quad \bar{\mathbf{D}}_b = \frac{2}{3} h_e \mathbf{C}_b^f + \frac{h_c^3}{12} \bar{\mathbf{C}}_b^c, \quad \bar{\mathbf{D}}_s = k \left(2h_f \mathbf{C}_s^f + h_c \bar{\mathbf{C}}_s^c \right), \quad (31)$$

in which (Jafari 2022)

$$\begin{aligned} \bar{\mathbf{C}}_b^c &= \begin{bmatrix} 3K_c \bar{\omega} \frac{(2+\bar{\omega})}{(1+2\bar{\omega})} & 3K_c \bar{\omega} \frac{(1-\bar{\omega})}{(1+2\bar{\omega})} & 0 \\ 3K_c \bar{\omega} \frac{(1-\bar{\omega})}{(1+2\bar{\omega})} & 3K_c \bar{\omega} \frac{(2+\bar{\omega})}{(1+2\bar{\omega})} & 0 \\ 0 & 0 & \frac{3K_c \bar{\omega}}{2} \end{bmatrix}, \\ \bar{\mathbf{C}}_s^c &= k \begin{bmatrix} 3/2 K_c \bar{\omega} & 0 \\ 0 & 3/2 K_c \bar{\omega} \end{bmatrix}, \quad \bar{\omega} = \frac{(c_1 + c_2) s + c_1 \lambda}{s + \lambda}. \end{aligned} \quad (32)$$

Defining

$$\bar{\mathbf{K}} = \int_A \mathbf{B}_p^T \bar{\mathbf{D}}_p \mathbf{B}_p dA + \int_A \mathbf{B}_b^T \bar{\mathbf{D}}_b \mathbf{B}_b dA + \int_A \mathbf{B}_s^T \bar{\mathbf{D}}_s \mathbf{B}_s dA, \tag{33}$$

$$\mathbf{K}_G = \int_A \mathbf{B}_G^T \mathbf{N}_p \mathbf{B}_G dA, \tag{34}$$

Equation (30) can be rewritten as follows:

$$\mathbf{U}^{xyT} \left(\bar{\mathbf{K}} - \mathbf{K}_G \right) \mathbf{F}^* \mathbf{U}^{xy} = 0. \tag{35}$$

Therefore,

$$\left| \bar{\mathbf{K}} - \mathbf{K}_G \right| = 0. \tag{36}$$

Equation (35) holds for every s , especially for $s = s_1$. Hence, one can write

$$\left| \bar{\mathbf{K}}_{s=s_1} - \mathbf{K}_G \right| = 0. \tag{37}$$

Finally, the power coefficient of the exponential time function s_1 is calculated by finding the minimum eigenvalue of Eq. (36).

To have a stable viscoelastic sandwich shell panel, we need $s_1 \leq 0$ ($|\alpha_1| < 1$). The critical condition in which $s_1 > 0$ is called viscoelastic or creep instability.

3 Numerical results

Matlab software is used to illustrate the proposed method. In the numerical results, the mechanical properties of the faces and the core are $E_f = 70$ GPa, $\nu_f = 0.34$, $K_c = 7$ GPa, $c_1 + c_2 = 1$. The shear correction factor is approximated as $k = 5/6$ for one-layer viscoelastic shells, and $k = 1$ for three-layer sandwich viscoelastic shells (Birman and Bert 2002). Regular distribution of $N = 11 \times 11$ scattered nodes is selected for calculating the time function coefficient based on the simple HP-cloud discretization.

3.1 Convergence study and verification

Table 1 shows a convergence study of stability analysis of simply supported elastic circular shell panels subjected to uniaxial in-plane load N_x . The local buckling coefficient is defined as $\hat{k} = \frac{b^2 N_{cr}}{\pi^2 D}$ in which $D = \frac{Eh^3}{12(1-\nu^2)}$ is the bending rigidity, and N_{cr} is the critical buckling load, $\frac{a}{b} = 1$, $\frac{h}{a} = 0.1$.

The results of Table 1 confirm the convergence related to the simple HP-cloud discretization method.

Table 2 compares the elastic buckling coefficients of simply supported spherical shells subjected to uniaxial and biaxial compressive loads according to the first-order shear deformation theory (FSDT) and higher-order shear deformation theory (HSDT). The proposed method results are obtained based on the $\alpha_1 = 1$ and the material property at time zero, $E(t = 0)$ and $\nu(t = 0)$. Other parameters used are $\frac{a}{b} = 1$, $\frac{h}{a} = 0.1$.

Table 3 compares the time function coefficient of simply supported viscoelastic plates having $\alpha_1 = 0$, $c_1 = 0.2$, $\frac{a}{b} = 1$, $\frac{h}{a} = 0.1$. To model the viscoelastic plate, viscoelastic shells with very large radii are considered.

As Tables 2–3 indicate, the results of the proposed method have good accuracy.

Table 1 Convergence study

	Distribution of nodes	$\hat{k} = \frac{b^2 N_{cr}}{\pi^2 D}$	
		$R = 1000, \alpha = 0.001$	$R = 20, \alpha = 0.05$
Circular shell analysis	$N = 9 \times 9$	3.720	3.744
	$N = 11 \times 11$	3.739	3.763
	$N = 13 \times 13$	3.755	3.779
	$N = 15 \times 15$	3.768	3.792
	$N = 17 \times 17$	3.781	3.805
Plate analysis	(Venkateswara et al. 1975)	3.7865	–
	(Hinton 1978)	3.737	–

Table 2 Compared buckling coefficients (\hat{k})

Geometrical properties	$\hat{k} = \frac{b^2 N_{cr}}{\pi^2 D}$			
	Uniaxial compression		Biaxial compression	
	Present (FSDT)	By Biswal et al. (2018) (HSDT)	Present (FSDT)	By Biswal et al. (2018) (HSDT)
$\frac{a}{R_1} = 0, \frac{b}{R_2} = 0$	3.7504	3.75	1.8775	1.8706
$\frac{a}{R_1} = 0.2, \frac{b}{R_2} = 0$	3.8500	3.85	1.9293	1.917
$\frac{a}{R_1} = 0.2, \frac{b}{R_2} = 0.2$	4.1976	4.165	2.1017	2.1017

Table 3 Compared time function coefficients (s_1)

Geometrical properties	s_1			
	$R_2/b = 1000$	$R_2/b = 10,000$	$R_2/b = 100,000$	By Eskandari et al. (2022)
Circular shell, $\frac{a}{R_1} = 0$	–0.2	–0.2	–0.2	–0.2
Spherical shell, $R_1 = R_2$	–0.2	–0.2	–0.2	–0.2

3.2 Time function coefficients of viscoelastic shell panels

Tables 4–6 show the time function coefficients of viscoelastic spherical shell panels with different material and geometrical properties subjected to uniaxial and biaxial compressions.

As Tables 4–6 indicate, by increasing the compressive force ratio α_1 , the time function coefficient s_1 is increased, while by increasing the constant part of relaxation function c_1 , s_1 is decreased.

It is noted that in cases $s_1 > 0$, positive numbers in Tables 4–6, the displacement exponentially grows, and creep instability occurs. So, it is necessary to limit the value of α_1 to prevent the viscoelastic instability. In other words, because of the time-dependent properties of viscoelastic materials, the maximum compression ratio α_1 must be checked by structural engineers. To have the stable condition, one needs $s_1 \leq 0$.

Table 4 Time function coefficients (s_1) of simply supported viscoelastic shells under different uniaxial compression ratios

$\frac{a}{b} = 1, \frac{b}{R_2} = 0.1, t_s = 1 s$		s_1					
		$\alpha_1 = 0$	$\alpha_1 = 0.1$	$\alpha_1 = 0.2$	$\alpha_1 = 0.3$	$\alpha_1 = 0.4$	$\alpha_1 = 0.5$
$\frac{h}{a} = 0.1, \frac{a}{R_1} = 0.1$	$c_1 = 0.1$	-0.10	-0.07	-0.03	+0.01	+0.05	+0.11
	$c_1 = 0.2$	-0.20	-0.17	-0.14	-0.11	-0.06	-0.01
	$c_1 = 0.3$	-0.30	-0.32	-0.25	-0.22	-0.18	-0.14
	$c_1 = 0.4$	-0.40	-0.38	-0.36	-0.33	-0.30	-0.26
$\frac{h}{a} = 0.1, \frac{a}{R_1} = 0.02$	$c_1 = 0.1$	-0.10	-0.07	-0.04	0.000	+0.05	+0.10
	$c_1 = 0.2$	-0.20	-0.17	-0.14	-0.11	-0.07	-0.02
	$c_1 = 0.3$	-0.30	-0.32	-0.25	-0.22	-0.18	-0.14
	$c_1 = 0.4$	-0.40	-0.38	-0.36	-0.33	-0.30	-0.26
$\frac{h}{a} = 0.1, \frac{a}{R_1} = 0$	$c_1 = 0.1$	-0.10	-0.07	-0.04	0.00	+0.050	+0.10
	$c_1 = 0.2$	-0.20	-0.17	-0.14	-0.11	-0.07	-0.02
	$c_1 = 0.3$	-0.30	-0.32	-0.25	-0.22	-0.18	-0.14
	$c_1 = 0.4$	-0.40	-0.38	-0.36	-0.33	-0.30	-0.26
$\frac{h}{a} = 0.15, \frac{a}{R_1} = 0.1$	$c_1 = 0.1$	-0.10	-0.06	-0.02	+0.02	+0.09	+0.16
	$c_1 = 0.2$	-0.20	-0.17	-0.13	-0.09	-0.04	+0.00
	$c_1 = 0.3$	-0.30	-0.27	-0.24	-0.20	-0.16	-0.10
	$c_1 = 0.4$	-0.40	-0.38	-0.35	-0.32	-0.28	-0.23

Table 5 Time function coefficients (s_1) of simply supported viscoelastic shells under different biaxial compression ratios

$k_1 = k_2 = 1, \frac{a}{R_1} = 0.1, \frac{a}{b} = 1, \frac{h}{a} = 0.1, t_s = 1 s$		s_1					
		$\alpha_1 = 0$	$\alpha_1 = 0.1$	$\alpha_1 = 0.2$	$\alpha_1 = 0.3$	$\alpha_1 = 0.4$	$\alpha_1 = 0.5$
$c_1 = 0.1$		-0.10	-0.08	-0.06	-0.03	-0.01	+0.02
$c_1 = 0.2$		-0.20	-0.18	-0.16	-0.14	-0.12	-0.09
$c_1 = 0.3$		-0.30	-0.31	-0.27	-0.25	-0.23	-0.20
$c_1 = 0.4$		-0.40	-0.39	-0.37	-0.36	-0.34	-0.32

Table 6 Time function coefficients (s_1) of clamped viscoelastic shells under different uniaxial compression ratios

$\frac{a}{R_1} = 0.1, \frac{a}{b} = 1, \frac{h}{a} = 0.1, t_s = 1 s$		s_1					
		$\alpha_1 = 0$	$\alpha_1 = 0.1$	$\alpha_1 = 0.2$	$\alpha_1 = 0.3$	$\alpha_1 = 0.4$	$\alpha_1 = 0.5$
$c_1 = 0.1$		-0.10	-0.05	0.00	+0.07	+0.15	+0.26
$c_1 = 0.2$		-0.20	-0.16	-0.11	-0.05	+0.03	+0.12
$c_1 = 0.3$		-0.30	-0.26	-0.22	-0.17	-0.10	-0.02
$c_1 = 0.4$		-0.40	-0.37	-0.33	-0.29	-0.23	-0.16

Besides, Tables 4–6 show that changing the geometrical properties, such as thickness-to-side ratio $\frac{h}{a}$, boundary conditions, and side-to-radius ratio $\frac{a}{R_1}$, has little effect on the time function coefficient of moderately thick viscoelastic shells.

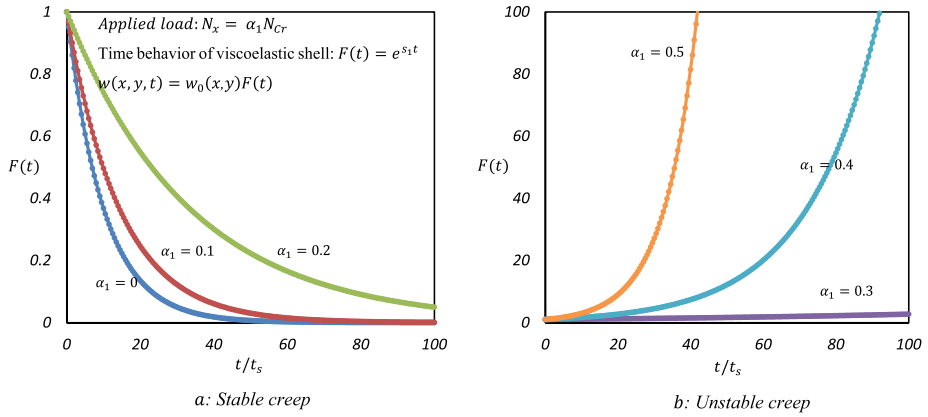


Fig. 2 $F(t)$ versus t/t_s under different uniaxial compression ratios

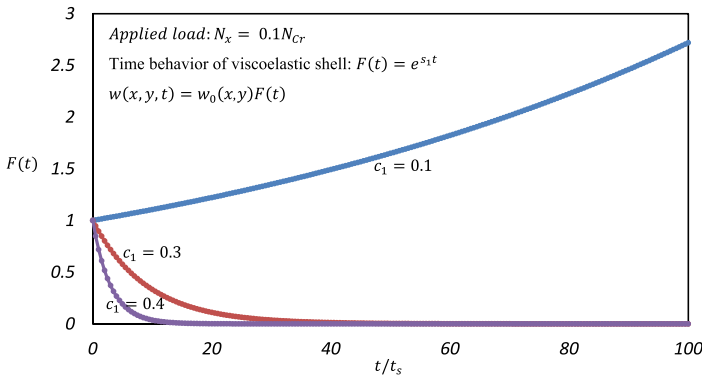


Fig. 3 $F(t)$ versus t/t_s with different material properties

Figure 2 compares two time-behaviors $F(t) = e^{s_1 t}$, namely stable creep $s_1 \leq 0$ and unstable creep $s_1 > 0$, of the simply supported viscoelastic spherical shell panel under different uniaxial in-plane compression ratios: $\alpha_1 = N_x/N_{Cr}$, $c_1 = 0.1$, $\frac{a}{b} = 1$, $\frac{b}{R_2} = \frac{a}{R_1} = 0.1$, $\frac{h_c}{a} = 0.1$, $\frac{h_f}{a} = 0$.

Figure 2(a) illustrates stable conditions $\alpha_1 = 0, 0.1, 0.2$ in which displacements are decreased and converge to zero as time increases, while Fig. 2(b) illustrates creep unstable conditions $\alpha_1 = 0.3, 0.4, 0.5$ in which displacements exponentially grow and diverge as time increases. So, it is necessary to limit the uniaxial compression considering the creep instability analysis.

Time behaviors of simply supported viscoelastic sandwich shells $F(t) = e^{s_1 t}$, with different material properties, are shown in Fig. 3, for $\alpha_1 = 0.1$, $\frac{a}{b} = 1$, $\frac{b}{R_2} = \frac{a}{R_1} = 0.1$, $\frac{h_c}{a} = 0.1$, $\frac{h_f}{a} = 0$.

As the results of Fig. 3 indicate, by increasing c_1 , the displacements converge to zero faster.

Table 7 Time function coefficients (s_1) of viscoelastic shells under different relaxation times

Material properties	s_1		
	$t_s = 0.1 \text{ s}$	$t_s = 1 \text{ s}$	$t_s = 10 \text{ s}$
$c_1 = 0.1$	-0.7	-0.07	-0.007
$c_1 = 0.2$	-1.73	-0.17	-0.017
$c_1 = 0.3$	-2.76	-0.28	-0.028
$c_1 = 0.4$	-3.78	-0.38	-0.038

Table 8 Time function coefficients (s_1) of viscoelastic shells under different tension and compression ratios

s_1						
$\alpha_1 = -0.8$	$\alpha_1 = -0.5$	$\alpha_1 = -0.3$	$\alpha_1 = 0$	$\alpha_1 = 0.3$	$\alpha_1 = 0.5$	$\alpha_1 = 0.8$
-0.72	-0.58	-0.47	-0.2	-0.05	+0.12	+0.21

Table 9 Time function coefficients (s_1) of viscoelastic sandwich shells under different uniaxial compression ratios

Geometrical properties	s_1				
	$\alpha_1 = 0$	$\alpha_1 = 0.1$	$\alpha_1 = 0.3$	$\alpha_1 = 0.5$	$\alpha_1 = 0.8$
$h_c = 0.06, h_f = 0.02$	-0.899	-0.896	-0.803	-0.677	-0.652
$h_c = 0.07, h_f = 0.015$	-0.817	-0.811	-0.680	0.585	-0.460
$h_c = 0.08, h_f = 0.01$	-0.738	-0.728	-0.490	-0.409	-0.360
$h_c = 0.09, h_f = 0.005$	-0.377	-0.364	-0.342	-0.305	-0.213
$h_c = 0.10, h_f = 0$	-0.20	-0.16	-0.05	+0.12	+0.21

Table 7 shows the time function coefficients of simply supported viscoelastic spherical shell panels with different relaxation times t_s , subjected to uniaxial compressions, $\alpha_1 = 0.1$, $\frac{a}{b} = 1, \frac{b}{R_2} = 0.1$.

Table 7 shows that the time function coefficients are linearly dependent on the relaxation times.

Table 8 illustrates the time function coefficients of simply supported viscoelastic spherical shells subjected to different uniaxial tensions $\alpha_1 < 0$ and compressions $\alpha_1 > 0$, for $c_1 = 0.2, \frac{a}{b} = 1, \frac{b}{R_2} = 0.1$.

As Table 8 indicates, by increasing α_1 , the time function coefficient is increased.

3.3 Time function coefficients of viscoelastic sandwich shell panels

Table 9 shows the time function coefficients of simply supported viscoelastic three-layer sandwich spherical shell panels with different material and geometrical properties under uniaxial compression ratios of $\frac{a}{R_1} = 0.1, \frac{a}{b} = 1, c_1 = 0.2$.

Table 9 shows that by increasing the thickness of the viscoelastic core layer, s_1 is increased, which confirms the damping effect of viscoelastic materials.

4 Conclusions

The creep instability analysis of time-dependent sandwich shell panels having elastic faces and viscoelastic cores was investigated in this paper. The creep instability of viscoelastic sandwich shell panels is related to the ratio of applied in-plane compressive load to the elastic buckling load at time zero, and the time-dependent viscoelastic material property, too.

The effect of material and geometrical parameters on the time behavior of viscoelastic sandwich shell panels subjected to in-plane compression was considered. Also, the maximum compressive load, which can be applied to the time-dependent sandwich shell panels without any creep instability, was determined.

Numerical results show that:

1. When $s_1 > 0$ (s_1 is the coefficient related to the time behavior of viscoelastic shells), the displacements exponentially grow, $w_0(x, y, t) = w_0(x, y)e^{s_1 t}$, and creep instability occurs. So, it is necessary to limit the maximum value of α_1 (α_1 is the compressive force ratio) to prevent viscoelastic instability and to have a stable condition.
2. In addition, by increasing the thickness of the viscoelastic core layer, s_1 is increased.
3. Also, by increasing c_1 (c_1 is the constant part of the relaxation function), the displacements converge to zero faster.

Author contributions Nasrin Jafari wrote the main manuscript and Mojtaba Azhari reviewed the manuscript.

Funding No funds, grants, or other support was received.

Data Availability No datasets were generated or analysed during the current study.

Declarations

Competing interests The authors declare no competing interests.

References

- Al-Furjan, M.S.H., Farrokhanian, A., Keshtegar, B., Kolahchi, R., Trung, N.T.: Higher order nonlocal viscoelastic strain gradient theory for dynamic buckling analysis of carbon nano cones. *Aerosp. Sci. Technol.* **107**, 106259 (2020). <https://doi.org/10.1016/j.ast.2020.106259>
- Birman, V., Bert, C.W.: On the choice of shear correction factor in sandwich structures. *J. Sandw. Struct. Mater.* **4**(1), 83–95 (2002). <https://doi.org/10.1177/1099636202004001180>
- Biswal, D.K., Mohanty, S.C.: On the static and dynamic stability of spherical sandwich shell panels with viscoelastic material core and laminated composite face sheets under uniaxial and biaxial harmonic excitations. *Acta Mech.* **231**, 1903–1918 (2020). <https://doi.org/10.1007/s00707-020-02618-6>
- Biswal, D.K., Joseph, S.V., Mohanty, S.C.: Free vibration and buckling study of doubly curved laminated shell panels using higher order shear deformation theory based on Sander's approximation. *J. Mech. Eng. Sci.* **232**(20), 3612–3628 (2018). <https://doi.org/10.1177/0954406217740165>
- Davidson, O.C., Browning, S.C.: An axially compressed cylindrical shell with a viscoelastic core. *AIAA J.* **2**(11) (1964). <https://doi.org/10.2514/3.2718>
- Drozdv, A.: Stability of viscoelastic shells under periodic and stochastic loading. *Mech. Res. Commun.* **20**(6), 481–486 (1993)
- Eskandari, M., Jafari, N., Azhari, M.: Time-dependent three-dimensional quasi-static analysis of a viscoelastic solid by defining a time function. *Mech. Time-Depend. Mater.* **26**(4), 829–856 (2022). <https://doi.org/10.1007/s11043-021-09515-y>
- Ferreira, A.J.M., Barbosa, J.T.: Buckling behavior of composite shells. *Compos. Struct.* **50**, 93–98 (2000). [https://doi.org/10.1016/S0263-8223\(00\)00090-8](https://doi.org/10.1016/S0263-8223(00)00090-8)

- Ganesan, S.N., Sethuraman, R.: Buckling and free vibrations of sandwich general shells of revolution with composite facings and viscoelastic core under thermal environment using semi-analytical method. *Comput. Model. Eng. Sci.* **18**(2), 121–144 (2007). <https://doi.org/10.3970/cmcs.2007.018.121>
- Hajmohammad, M.H., Azizkhani, M.B., Kolahchi, R.: Multiphase nanocomposite viscoelastic laminated conical shells subjected to magneto-hygrothermal loads: dynamic buckling analysis. *Int. J. Mech. Sci.* **137**, 205–213 (2018). <https://doi.org/10.1016/j.ijmecsci.2018.01.026>
- Hinton, E.: Buckling of initially stressed Mindlin plates using a finite strip method. *Comput. Struct.* **8**(1), 99–105 (1978). [https://doi.org/10.1016/0045-7949\(78\)90164-5](https://doi.org/10.1016/0045-7949(78)90164-5)
- Ishakov, V.I.: Stability analysis of viscoelastic thin shallow hyperbolic paraboloid shells. *Int. J. Solids Struct.* **36**(28), 4209–4223 (1999). [https://doi.org/10.1016/S0020-7683\(98\)00197-8](https://doi.org/10.1016/S0020-7683(98)00197-8)
- Jafari, N.: Time-dependent p-delta analysis of Timoshenko viscoelastic beams and Mindlin viscoelastic plates with different shapes. *Structures* **43**, 1436–1446 (2022). <https://doi.org/10.1016/j.istruc.2022.07.072>
- Jafari, N., Azhari, M.: Buckling of moderately thick arbitrarily shaped plates with intermediate point supports using a simple hp-cloud method. *Appl. Math. Comput.* **313**, 196–208 (2017). <https://doi.org/10.1016/j.amc.2017.05.079>
- Jafari, N., Azhari, M.: On the viscoelastic instability of Timoshenko viscoelastic beams and Mindlin viscoelastic plates under compressive loads. *Mech. Time-Depend. Mater.* (2022). <https://doi.org/10.1007/s11043-022-09580-x>
- Li, Y.S., Liu, B.L.: Thermal buckling and free vibration of viscoelastic functionally graded sandwich shells with tunable auxetic honeycomb core. *Appl. Math. Model.* **108**, 685–700 (2022). <https://doi.org/10.1016/j.apm.2022.04.019>
- Liu, T., Chen, Y., Hutchinson, J.W., Jin, L.: Buckling of viscoelastic spherical shells. *J. Mech. Phys. Solids* **169**, 105084 (2022). <https://doi.org/10.1016/j.jmps.2022.105084>
- Mahmoudkhani, S., Sadeghmanesh, M., Haddadpour, H.: Aero-thermo-elastic stability analysis of sandwich viscoelastic cylindrical shells in supersonic airflow. *Compos. Struct.* **147**(1), 185–196 (2016). <https://doi.org/10.1016/j.compstruct.2016.03.020>
- Peng, F., Liu, Y., Fu, Y.: Analysis of critical axially compressive loads for viscoelastic laminated circular cylindrical shells. *Chin. J. Theor. Appl. Mech.* **23**(5), 626–632 (2007). <https://doi.org/10.6052/0459-1879-2007-5-2006-536>
- Pradeep, V., Ganesan, N., Padmanabhan, C.: Buckling and vibration behavior of a viscoelastic sandwich cylinder under thermal environment. *Int. J. Comput. Methods Eng. Sci. Mech.* **7**(5), 389–401 (2006). <https://doi.org/10.1080/15502280600790413>
- Reddy, J.N.: *Mechanics of Laminated Composite Plates and Shells*. CRC Press, Boca Raton (2004). <https://doi.org/10.1201/b12409>
- Tylikowski, A.: Dynamic stability of viscoelastic shells under time-dependent membrane loads. *Int. J. Mech. Sci.* **31**(8), 591–597 (1989). [https://doi.org/10.1016/0020-7403\(89\)90066-0](https://doi.org/10.1016/0020-7403(89)90066-0)
- Venkateswara, G.R., Venkataramana, J., Kanaka, K.R.: Stability of moderately thick rectangular plates using a high precision triangular finite element. *Comput. Struct.* **5**, 257–259 (1975). [https://doi.org/10.1016/0045-7949\(75\)90028-0](https://doi.org/10.1016/0045-7949(75)90028-0)
- Vinogradov, A.M.: Creep-stability analysis of viscoelastic cylindrical shells. *Math. Model.* **7**, 529–536 (1986). [https://doi.org/10.1016/0270-0255\(86\)90071-0](https://doi.org/10.1016/0270-0255(86)90071-0)
- Xu, S., Gao, H., Qiu, P., et al.: Stability analysis of acrylic glass pressure cylindrical shell considering creep effect. *Thin-Walled Struct.* **181**, 110033 (2022). <https://doi.org/10.1016/j.tws.2022.110033>

Publisher's Note Springer Nature remains neutral with regard to jurisdictional claims in published maps and institutional affiliations.

Springer Nature or its licensor (e.g. a society or other partner) holds exclusive rights to this article under a publishing agreement with the author(s) or other rightsholder(s); author self-archiving of the accepted manuscript version of this article is solely governed by the terms of such publishing agreement and applicable law.